Modelling and Control of Doubly Fed Induction Generator based stand-alone Wind Energy Conversion System

A THESIS SUBMITTED IN PARTIAL FULFILLMENT OF THE REQUIREMENT FOR THE DEGREE OF

Master of Technology

In

Electrical Engineering

By

KOTA VINAY KUMAR REDDY

Roll No. 213EE4334

Department of Electrical Engineering

National Institute of Technology Rourkela

Rourkela-769008

Modelling and Control of Doubly Fed Induction Generator based stand-alone Wind Energy Conversion System

A THESIS SUBMITTED IN PARTIAL FULFILLMENT OF THE REQUIREMENTS FOR THE DEGREE OF

Master of Technology

In

Electrical Engineering

By

KOTA VINAY KUMAR REDDY

Under the guidance of

Prof. MONALISA PATTNAIK

Department of Electrical Engineering

National Institute of Technology Rourkela

Rourkela-769008

Department of Electrical Engineering
National Institute of Technology Rourkela

Certificate

This is to certify that the thesis entitled, "**Modelling and Control of Doubly Fed Induction Generator based stand-alone Wind Energy Conversion System**" submitted by Mr. Kota Vinay Kumar Reddy in partial fulfillment of the requirements for the award of Master of Technology Degree in **Electrical Engineering** with specialization in "**Power Electronics and Drives**" during session 2013-15 at National Institute of Technology, Rourkela is an authentic work carried out by him under my supervision and guidance. This work has not been submitted at other University/ Institute for the award of any degree or diploma.

Date:

Place:

<div align="right">

Prof. Monalisa Pattnaik

Department of Electrical Engineering

National Institute of Technology

Rourkela-769008

</div>

Acknowledgement

I would like to express my sincere gratitude to my supervisor Prof. Monalisa Pattnaik for her guidance, encouragement, and support throughout the course of this work. It was an invaluable learning experience for me to be one of her students. As my supervisor her insight, observations and suggestions helped me to establish the overall direction of the research and contributed immensely for the success of this work.

I express my gratitude to Prof. A. K. Panda, Head of the Department, Electrical Engineering for his invaluable suggestions and constant encouragement all through this work. My thanks are extended to my colleagues in power control and drives, who built an academic and friendly research environment that made my study at NIT, Rourkela most fruitful and enjoyable. I would also like to acknowledge the entire teaching and non-teaching staff of Electrical department for establishing a working environment and for constructive discussions. Finally, I am always indebted to all my family members, especially my parents, for their endless support and love.

Last but not least I would like to thank my parents, who taught me to work hard by their own example. They provided me much support being apart during the whole tenure of my stay in NIT Rourkela.

Kota Vinay Kumar Reddy

ROLL NO. - 213EE4334

Abstract

The application of wound rotor induction machine is widely spread in wind energy generating stations because of its adaptability for variable speed wind turbines through which maximum possible extraction of wind energy is possible. Also among all the induction generator configurations for wind power systems the use of Doubly Fed Induction Generator (DFIG) configuration with back to back pulse width modulated voltage source converters (VSC) is one of the best topologies available and it is suitable for both grid connected systems as well as stand-alone systems. Here only stand-alone application of DFIG is considered. In this thesis mathematical modelling of doubly fed induction machine is presented. The control strategies for both stator side converter and rotor side converter are developed in stator flux oriented reference frame. The dynamics of dc link voltage build-up phase is also included. The stator side converter is used to control the output voltage in direct voltage control manner and the rotor side converter is current controlled where the power imbalance of the system is nullified using dc link voltage controller which modifies the quadrature axis rotor current reference value according to the changes in the wind speed as well as the load. Two control algorithms are presented out of which one gives the best performance for all kinds of loads (balance, unbalance, linear and non-linear) and the other gives poor load regulation and unwanted distortions in the output voltage for non-linear and unbalanced loads.

Table of Contents

List of figures

List of Abbreviations

DFIG	Doubly-Fed Induction Generator
IGBT	Insulated Gate Bipolar Transistor
PMSG	Permanent Magnet Synchronous Generator
PWM	Pulse Width Modulation
PI	Proportional and Integral
SPWM	Sinusoidal Pulse Width Modulation
SVPWM	Space Vector Pulse Width Modulation
VSC	Voltage Source Converter
VSCF	Variable Speed Constant Frequency
VSI	Voltage Source Inverter
WECS	Wind Energy Conversion Systems
WTGS	Wind Turbine Generating Systems
WRIM	Wound Rotor Induction Machine

CHAPTER 1

INTRODUCTION

As the availability of conventional energy resources is going down day by day there is a serious need for use of alternate renewable sources such as solar cells, wind turbines, hydro power and biomass etc. There are many engineers and several institutes responsible for making optimal utilization of all these non-conventional energy sources possible.

Out of all the above mentioned sources wind power has its own importance because of the various advancements and improved performance of several Wind Energy Conversion Systems (WECS). Most of the global energy is being increasingly generated by modern wind power systems. Germany is among the biggest wind power markets. Along with Germany there are many countries like US, Spain, France, Denmark, China and India as well which considers wind energy as a serious alternate for generation of electricity. Because of this a major focus is kept on wind power conversion systems in the current thesis.
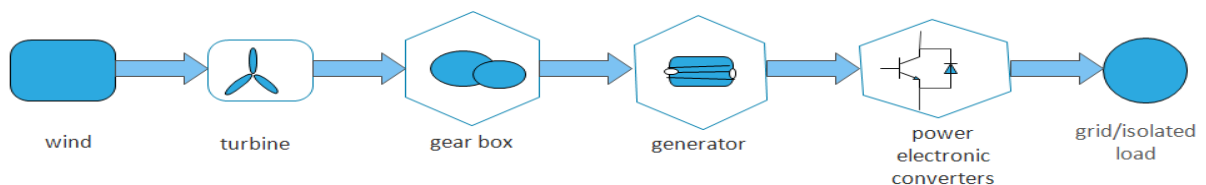
Fig. 1.1 Components of WECS scheme.

Different stages of a wind power generating system consisting of electro mechanical energy conversion devices, electrical components, mechanical components and aerodynamic components is shown in Fig. 1.1.

1.1   IMPORTANCE OF DFIG IN WECS

All the wind turbines used can be majorly categorized in to the following two types. Fixed speed wind turbines and variable speed wind turbines. In fixed speed wind turbines the electromechanical energy conversion device used can be of synchronous machine type where there will be a mechanical speed control through gear ratio in between the wind turbine and the machine shaft. This leads to increased mechanical losses which in turn reduces the efficiency of the overall energy conversion process. On the other hand a partial variable speed wind turbine uses asynchronous machine for mechanical energy to electrical energy conversion which can automatically vary its rotor slip for variations in wind speed. Also a Doubly Fed Induction Generator (DFIG) with ac-dc-ac converter in between stator and rotor windings is adaptable for variable speed wind turbines without any gear ratio control. This topology has distinct advantages where the speed range can be extended on both sides of synchronous speed depending on the voltage rating of the rotor. Also as the power electronic converter used here is of lower rating as it has to deal only with the slip power, the converter losses will be low and the cost will also become less. There are some more advantages like the harmonic injection will be low if it is grid connected operation. On the other hand a Permanent Magnet Synchronous Generator (PMSG) can be used with a power electronic converter rated at the machine level. In this topology the output terminals are connected to the power grid via a power converter which is rated at the generator power level. Sometimes a direct driven multipole machine is considered for gearless operation.

All in all a wind turbine with varying speed is considered more effective compared to that of a wind turbine which rotates at a particular fixed speed because of several disadvantages of fixed speed turbines like high mechanical stress during wind gusts and so on. In the current thesis more emphasis is thrown only on DFIG based variable speed Wind Turbine Generating Systems (WTGS). Also there are several advantages of DFIG based systems compared to PMSG generating systems some of which are listed as follows.

1. Construction of DFIG is robust and is comparatively less costly than PMSG.
2. Power can be generated from stator as well as rotor which results in higher output power.
3. In DFIG based WTGS the power converter is typically rated around thirty percent of the rated power which makes the entire system to be cost effective and gives an overall improved performance.

Even though the DFIG system needs regular maintenance and has complex control structures compared to PMSG, they are widely used in wind turbine industry for large rated systems. Hence only DFIG systems will be focused here along with the mathematical modelling and control structures for DFIG based stand-alone WECS system. The major reason behind consideration of stand-alone system is that in some remote parts of the world it is very difficult to maintain electrical supply through power grid because of economical and operational difficulties. Therefore in those areas wind energy based stand-alone systems can be used to supply regional loads based on their geographical location. Hence DFIG systems operating in stand-alone mode are emphasized.

1.2 LITERATURE SURVEY

This section gives a brief review of various literatures available on DFIG based wind turbine generating systems. To be more precise it consist of study carried out by many researchers on

modelling, control schemes and different power electronic converter topologies used in DFIG based WTGS.

- DFIG modelling

  In wind turbine generator systems the standard type DFIG and brushless type DFIG are mostly used. In reference [1] brushless DFIG employed with two cascaded induction machines is developed and a closed loop control scheme designed in stator flux orientation is used for commanding the active power along with the reactive power. In [2] and [3] authors considered synchronously rotating reference frame for design of control strategies because of its capability of reducing the complexity by converting the alternating quantities in to dc quantities. In [3] the author considered a third order model consisting of direct current components of stator currents and compared with a full order model under different wind speed situations. In [4] the author proposed a new third order model without considering resistance and inductance of stator winding and compared with a full order model for transient performance. Due to similarity between Squirrel Cage Induction Generator (SCIG) and DFIG the difference being that the rotor winding terminals are available for external connection in case of DFIG the simplified models of squirrel cage induction generator can sometimes come in handy for understanding the modelling of DFIG and interested readers can find them in [5] and [6].

- Power converter modelling

  A back to back PWM converter topology is mostly used in DFIG based WTGS irrespective to the mode of operation of the system. In [7] the author deduced the mathematical model expressed in ABC reference frame based on space vectors. The elaborative work regarding

modelling of PWM converter along with changing the axis from ABC to dqO is shown in [8]-[10].

- Control strategy for DFIG based stand-alone WECS

  There are several literatures available regarding DFIG based wind energy systems. The operation of grid connected DFIG systems is more extensively presented in the initial stages of research on DFIG based wind energy systems. The authors explained grid connected DFIG based WECS with different control structures in references [11]-[13]. Less attention is paid for stand-alone DFIG based systems in the initial stages but R. Pena et.al [14] proposed the design of such systems where stator flux is forced to align with a reference frame which is predefined and also rotates at constant angular frequency. The major issue here is that during sudden disturbances at the stator terminals the field orientation is not properly achieved resulting in unwanted transients in the output voltage. Speed sensor less control strategy using direct control method is proposed in [15]-[16]. The control strategy proposed is load dependent and transient results are shown for only resistive load. In [17] the authors proposed a new control algorithm where the voltage at the output terminals is governed by open loop scheme and also included the analysis of rise of voltage at the dc link capacitor terminals. A new control strategy for maintaining constant magnitude and fixed frequency voltage profile regardless to the sudden changes in load along with the speed variation is proposed in [18] and the evaluation for different load categories is also included in reference [18].

1.3   MOTIVATION

In some remote places it is difficult to maintain power supply through grid because of economical and operation difficulties. In such places depending on their geographical location and availability

of wind energy DFIG based stand-alone wind energy conversion systems can be adopted to supply the regional loads. Also this topology results in higher output power if the speed is above synchronous speed.

The power converters that are used in DFIG based systems are required to handle only part of the overall machine power rating which leads to several advantages like lower converter losses and also results in an overall cost effective system. Also DFIG based stand-alone WECS can be designed with a capability of feeding all types of loads.

1.4   OBJECTIVES

The following includes the major objectives of this project work.

- To maintain constant magnitude and constant frequency voltage profile at the generator terminals irrespective of load variation and changes in prime mover speed.
- To achieve improved transient performance of the entire system during load transients and changes in prime mover speed.
- To get satisfactory operation of the developed model for different load categories which might include an unbalanced nonlinear load as well.

1.5   THESIS ORGANISATION

This entire thesis consists of five chapters along with this current introductory chapter. In the second chapter mathematical modelling of DFIG is presented which includes the dynamic models of induction machine in several reference frames along with active power, reactive power and torque calculation. In the third chapter a control algorithm for DFIG based WECS in stand-alone mode is presented which majorly concerns the output voltage and frequency control. It controls

the output voltage in direct voltage control manner in open loop mode i.e. without any feedback from output side. This control strategy is tested for linear and nonlinear loads where it gives poor load voltage regulation and unwanted distortions in the load voltage profile for nonlinear loads. In the fourth chapter a different control algorithm is presented which controls the output voltage in closed loop manner which include stator voltage controllers. This model is tested for all kinds of loads and it gives satisfactory results for nonlinear loads as well without any distortions in the load voltage. In the last chapter i.e. in fifth chapter conclusions and scope for further studies are presented.

MATHEMATICAL MODEL OF DFIG

In wind energy generation systems the power extraction and conversion process is majorly done in two steps. In first step the kinetic energy possessed by wind is converted in to mechanical energy using aero-dynamics and turbines. The second step is carried out by electrical generator which is DFIG in the present system. In order to examine the various issues associated with stand-alone WECS, a proper model of the system should be established first.

In this chapter wind energy conversion system is introduced first and then a complete focus is given for DFIG model expressed in stationary ABC reference frame and dynamic models of DFIG in rotating reference frames are established using the classical transformations.

2.1 INTRODUCTION

The schematic of stand-alone variable speed WECS is shown in Fig. 2.1. The stator winding terminals are connected to the load via a filter and back to back VSC converters are connected between stator and rotor terminals which is clear from the schematic diagram in Fig. 2.1. These converters are bidirectional converters made of Insulated Gate Bipolar Transistor (IGBT) switches with anti-back diodes connected in parallel across each switch which makes the flow of bidirectional current possible. The control system that governs the stator and rotor converters are designed to achieve the desired objectives and to control the dynamic performance of the system.
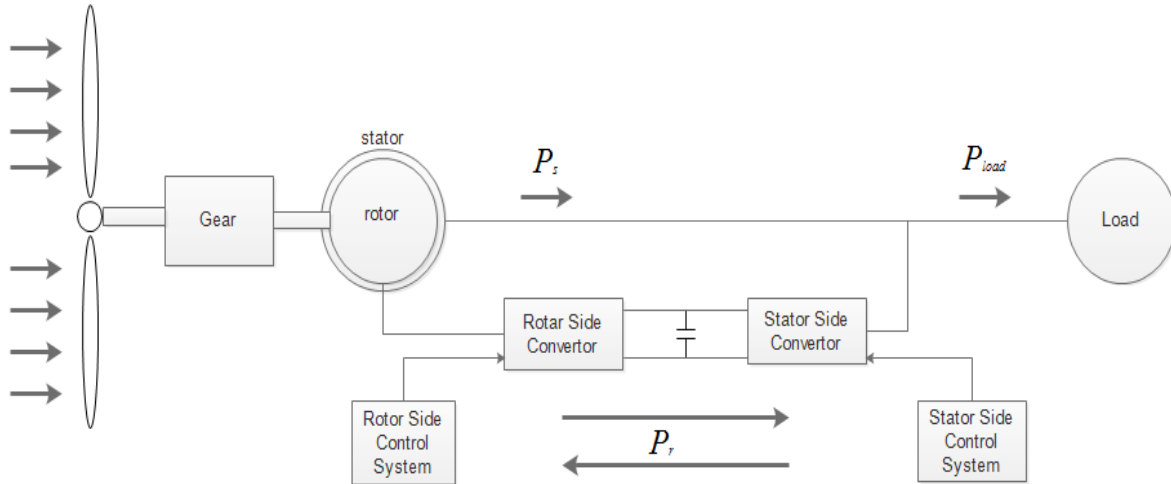
Fig. 2.1 Schematic of DFIG based WECS

The two converters are named as stator converter and rotor converter with a capacitor connected in between them as described in Fig. 2.1. The converter in the load side is controlled to get the desired output voltage profile and the converter in the machine side is controlled to maintain power balance of the system by governing the voltage at dc link capacitor.

2.2 DFIG MODELS

Design of vector control principles demands better understanding of the machine transient behavior which can be done using the study of dynamic models of the machine. The mathematical representation of machine that is necessary for control structure design should include all the dynamic effects that comes in to picture while the model is in steady state and transient mode [19]. Such a model which is effective for all the arbitrary and instantaneous variations in both voltages and currents and also that describes the machine under transients along with steady state is presented in this current section.

2.2.1 MODEL OF DFIG IN ABC REFERENCE FRAME

A simple two pole three phase slip ring induction machine is considered for mathematical modelling. The schematic of the machine in its cross sectional view is shown in Fig. 2.2.
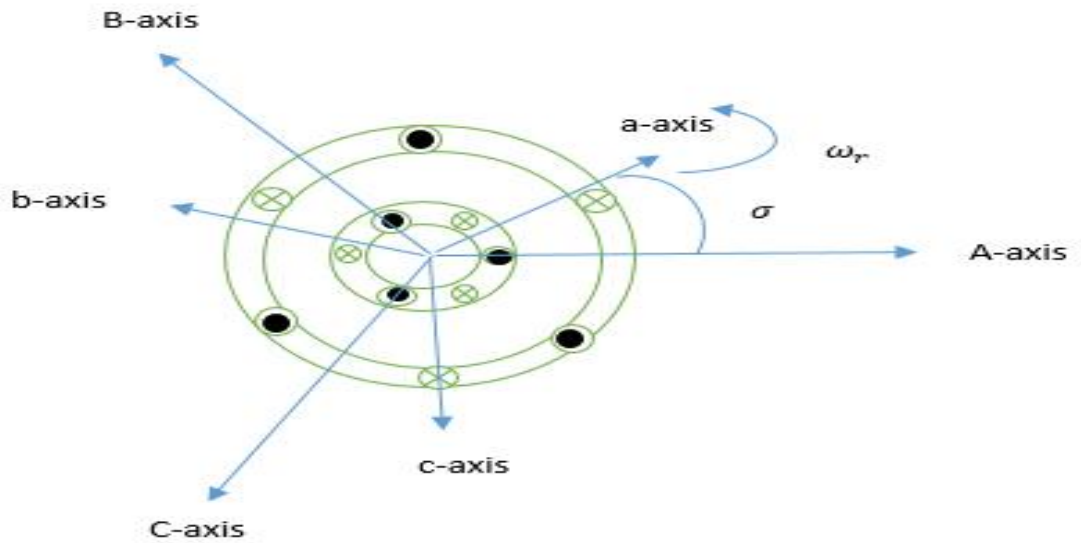
Fig. 2.2 Cross sectional view of WRIM

The machine is characterized by the following assumptions as mentioned below [19]:

1 Air gap is uniform.

2 Saturation effect is neglected.

3 Three phase windings are uniformly distributed so that per phase resistance and inductance is same for all the three phases.

4 The distribution of flux is sinusoidal along the air gap periphery.

5 Core losses are neglected and only resistive drops are considered.

Each phase is considered by means of a single coil due to the resemblance of all the three phases. That is each phase winding of the machine is represented with the help of a single coil as shown in Fig. 2.2. The subscripts 'A, B and C' are used to represent stator quantities and 'a, b and c' represent rotor quantities. The coils representing stator windings are A, B and C and their corresponding voltages are presented as follows:

$$v_A = r_A i_A + \frac{d}{dt}(\psi_A) \tag{2.1}$$

Where

$$\psi_A = (L_{AA} i_A + L_{AB} i_B + L_{AC} i_C + L_{Aa} i_a + L_{Ab} i_b + L_{Ac} i_c) \tag{2.2}$$

i.e.

$$v_A = r_A i_A + \frac{d}{dt}(L_{AA} i_A + L_{AB} i_B + L_{AC} i_C + L_{Aa} i_a + L_{Ab} i_b + L_{Ac} i_c) \tag{2.3}$$

Similarly the expressions for the other two stator voltages are written below

$$v_B = r_B i_B + \frac{d}{dt}(L_{BA} i_A + L_{BB} i_B + L_{BC} i_C + L_{Ba} i_a + L_{Bb} i_b + L_{Bc} i_c) \tag{2.4}$$

$$v_C = r_C i_C + \frac{d}{dt}(L_{CA} i_A + L_{CB} i_B + L_{CC} i_C + L_{Ca} i_a + L_{Cb} i_b + L_{Cc} i_c) \tag{2.5}$$

$$r_A = r_B = r_C = r_S \tag{2.6}$$

The coils representing rotor windings are a, b, and c and their corresponding voltage equations are given below

$$v_a = r_a i_a + \frac{d}{dt}(L_{aa} i_a + L_{ab} i_b + L_{ac} i_c + L_{Aa} i_A + L_{Ba} i_B + L_{Ca} i_C) \tag{2.7}$$

$$v_b = r_b i_b + \frac{d}{dt}(L_{ba} i_a + L_{bb} i_b + L_{bc} i_c + L_{Ab} i_A + L_{Bb} i_B + L_{Cb} i_C) \tag{2.8}$$

$$v_c = r_c i_c + \frac{d}{dt}(L_{ca}i_a + L_{cb}i_b + L_{cc}i_c + L_{Ac}i_A + L_{Bc}i_B + L_{Cc}i_C) \tag{2.9}$$

The resistance of each phase winding of the rotor is assumed to be equal and let it be denoted by $'r_r'$.

$$L_{AA} = L_{BB} = L_{CC} = L_{SS} \tag{2.10}$$

$$L_{AB} = L_{BC} = L_{CA} = L_{SM} \tag{2.11}$$

$$L_{aa} = L_{bb} = L_{cc} = L_{rr} \tag{2.12}$$

$$L_{ab} = L_{bc} = L_{ca} = L_{rm} \tag{2.13}$$

All the above inductive coefficients are not time variant as the displacement between the corresponding windings is always fixed irrespective of the rotor winding position. Now coming to the mutual inductance terms between stator and rotor windings, they are time variant as the rotor winding is changing its angular position with respect to time. The expressions for these coefficients are functions of the angular position of the rotor which are given below

$$L_{Aa} = L_{Bb} = L_{Cc} = L_{rsm}\cos(\sigma) \tag{2.14}$$

$$L_{Ab} = L_{Bc} = L_{Ca} = L_{rsm}\cos(\sigma + {}^{2\pi}/_3) \tag{2.15}$$

$$L_{Ac} = L_{Ba} = L_{Cb} = L_{rsm}\cos(\sigma - {}^{2\pi}/_3) \tag{2.16}$$

Where L_{rsm} indicates the inductance that is mutual for stator and rotor windings which is maximum and σ is the angle shown in Fig. 2.2. The mathematical model describing a WRIM in ABC reference frame is shown in matrix form in equation (2.17).

$$\begin{bmatrix} V_A \\ V_B \\ V_C \\ \cdots \\ V_a \\ V_b \\ V_c \end{bmatrix} = \begin{bmatrix} r_s & 0 & 0 & \vdots & 0 & 0 & 0 \\ 0 & r_s & 0 & \vdots & 0 & 0 & 0 \\ 0 & 0 & r_s & \vdots & 0 & 0 & 0 \\ \cdots & \cdots & \cdots & \vdots & \cdots & \cdots & \cdots \\ 0 & 0 & 0 & \vdots & r_r & 0 & 0 \\ 0 & 0 & 0 & \vdots & 0 & r_r & 0 \\ 0 & 0 & 0 & \vdots & 0 & 0 & r_r \end{bmatrix} \begin{bmatrix} I_A \\ I_B \\ I_C \\ \cdots \\ I_a \\ I_b \\ I_c \end{bmatrix}$$

$$+ \frac{d}{dt} \begin{bmatrix} L_{ss} & L_{sm} & L_{sm} & \vdots \\ L_{sm} & L_{ss} & L_{sm} & \vdots \\ L_{sm} & L_{sm} & L_{ss} & \vdots \\ \cdots \cdots & \cdots \cdots & \cdots \cdots & \vdots \\ L_{rsm}\cos(\sigma) & L_{rsm}\cos(\sigma + {}^{4\pi}/_3) & L_{rsm}\cos(\sigma + {}^{2\pi}/_3) & \vdots \\ L_{rsm}\cos(\sigma + {}^{2\pi}/_3) & L_{rsm}\cos(\sigma) & L_{rsm}\cos(\sigma + {}^{4\pi}/_3) & \vdots \\ L_{rsm}\cos(\sigma + {}^{4\pi}/_3) & L_{rsm}\cos(\sigma + {}^{2\pi}/_3) & L_{rsm}\cos(\sigma) & \vdots \end{bmatrix}$$

$$\begin{bmatrix} \vdots & L_{rsm}\cos(\sigma) & L_{rsm}\cos(\sigma + {}^{2\pi}/_3) & L_{rsm}\cos(\sigma + {}^{4\pi}/_3) \\ \vdots & L_{rsm}\cos(\sigma + {}^{4\pi}/_3) & L_{rsm}\cos(\sigma) & L_{rsm}\cos(\sigma + {}^{2\pi}/_3) \\ \vdots & L_{rsm}\cos(\sigma + {}^{2\pi}/_3) & L_{rsm}\cos(\sigma + {}^{4\pi}/_3) & L_{rsm}\cos(\sigma) \\ \vdots & \cdots \cdots & \cdots \cdots & \cdots \cdots \\ \vdots & L_{rr} & L_{rm} & L_{rm} \\ \vdots & L_{rm} & L_{rr} & L_{rm} \\ \vdots & L_{rm} & L_{rm} & L_{rr} \end{bmatrix} \begin{bmatrix} I_A \\ I_B \\ I_C \\ \cdots \\ I_a \\ I_b \\ I_c \end{bmatrix} \qquad (2.17)$$

Form the above matrix form it is clear that inductance matrix is time variant which depends on position of the rotor. So in order to reduce the complexity involved with time varying quantities dqo reference frames are preferred to model induction machine which transforms the time varying quantities in to constant quantities and thus results in constant voltages and currents along with constant inductive coefficients.

2.2.2 MODEL OF DFIG IN STATIONARY REFERENCE FRAME

As seen in the above section where DFIG model is expressed in ABC reference frame the coefficients of mutual inductance terms are varying in nature which makes it difficult for the analysis of the machine. Hence classical transformations came in to picture which makes these coefficients to remain constant by making all the rotor and stator windings to remain at a constant angular displacement at all times. This is possible by converting the rotor and stator windings in to two phase equivalent virtual windings which are stationary to each other. Using this transformation concept the dynamic model of WRIM is developed in a synchronously rotating reference frame and stationary reference frame as well. In the current section dynamic model of induction machine in stationary reference frame is presented.
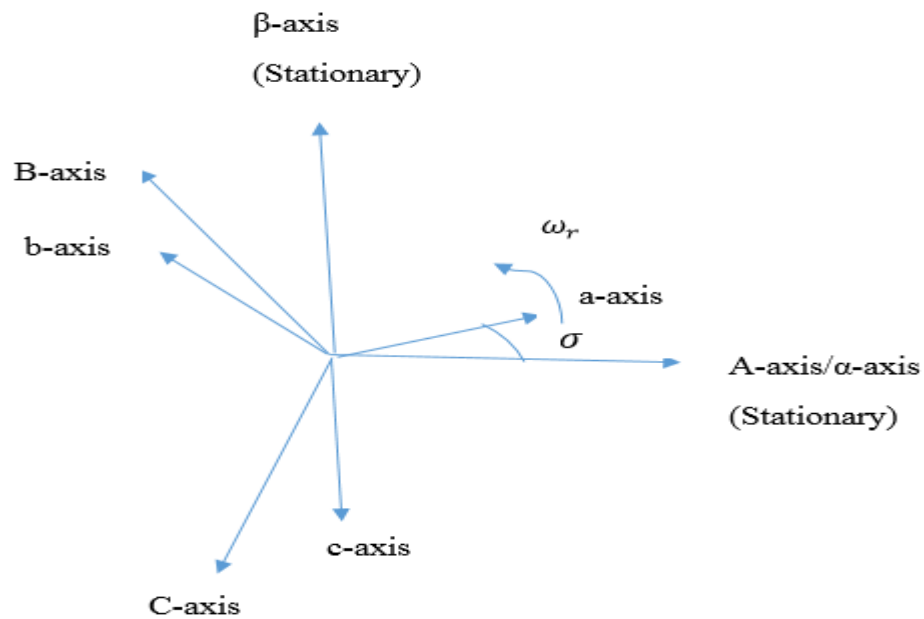

Fig. 2.3 Schematic of axis transformation (ABC to αβ).

Consider the diagram shown in Fig. 2.3 where the stationary α-axis is assumed to be aligned with the magnetic axis of stator phase A winding. Now let us assume that the stator and rotor variables

are transformed in to α-β axes which are stationary as shown in Fig. 2.3. The corresponding transformation matrices can easily be derived as follows. Let M_{sst} and M_{rst} indicate the matrices for transforming stator and rotor quantities respectively which are given as follows [20]:

$$M_{sst} = \frac{2}{3}\begin{bmatrix} 1 & -\frac{1}{2} & -\frac{1}{2} \\ 0 & \frac{\sqrt{3}}{2} & -\frac{\sqrt{3}}{2} \\ \frac{1}{2} & \frac{1}{2} & \frac{1}{2} \end{bmatrix}$$

(2.18)

$$M_{rst} = \frac{2}{3}\begin{bmatrix} \cos(\sigma) & \cos(\sigma + \frac{2\pi}{3}) & \cos(\sigma + \frac{4\pi}{3}) \\ \sin(\sigma) & \sin(\sigma + \frac{2\pi}{3}) & \sin(\sigma + \frac{4\pi}{3}) \\ \frac{1}{2} & \frac{1}{2} & \frac{1}{2} \end{bmatrix}$$

(2.19)

The final voltage and flux linkage equations that represent the dynamic model of induction machine in stationary reference frame (α-β) are given below (2.20)-(2.27).

$$v_{\alpha s} = r_s i_{\alpha s} + \frac{d}{dt}\psi_{\alpha s}$$

(2.20)

$$v_{\beta s} = r_s i_{\beta s} + \frac{d}{dt}\psi_{\beta s}$$

(2.21)

$$v_{\alpha r} = r_r i_{\alpha r} + \frac{d}{dt}\psi_{\alpha r} + \omega_r \psi_{\beta r}$$

(2.22)

$$v_{\beta r} = r_r i_{\beta r} + \frac{d}{dt}\psi_{\beta r} - \omega_r \psi_{\alpha r}$$

(2.23)

$$\psi_{\alpha s} = L_s i_{\alpha s} + L_m i_{\alpha r}$$

(2.24)

$$\psi_{\beta s} = L_s i_{\beta s} + L_m i_{\beta r}$$

(2.25)

$$\psi_{\alpha r} = L_r i_{\alpha r} + L_m i_{\alpha s}$$

(2.26)

$$\psi_{\beta r} = L_r i_{\beta r} + L_m i_{\beta s}$$

(2.27)

2.2.3 MODEL OF DFIG IN SYNCHRONOUS REFERENCE FRAME

The model of WRIM expressed in d-q reference frame rotating at synchronous speed is derived by considering the axis position as shown in Fig. 2.4. Synchronously rotating d-axis is shown at an angle of σ_s ahead of stator phase A winding axis and rotor phase a coil axis is σ ahead of stator phase A coil axis. Let ω_s be the synchronous speed with which d-q axes rotate.
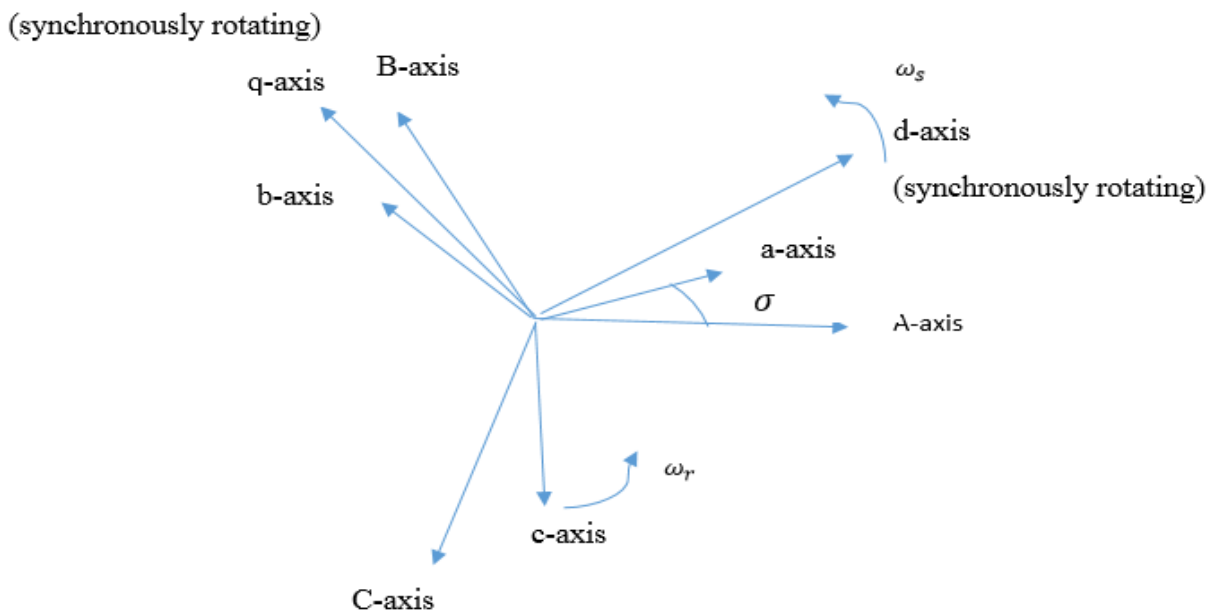

Fig. 2.4 Schematic of axis transformation (ABC to dq).

As explained in the previous cases the transformation matrices for transforming the stator and rotor variables are derived by projecting them on to d-q axes considering the schematic in Fig. 2.4. Let M_s and M_r be the transformation matrices for stator and rotor quantities respectively. These matrices are given in the following equations (2.28)-(2.29).

$$M_s = \frac{2}{3}\begin{bmatrix} \cos(\sigma_s) & \cos(\sigma_s - 2\pi/3) & \cos(\sigma_s - 4\pi/3) \\ -\sin(\sigma_s) & -\sin(\sigma_s - 2\pi/3) & -\sin(\sigma_s - 4\pi/3) \\ 1/2 & 1/2 & 1/2 \end{bmatrix} \tag{2.28}$$

$$M_r = \frac{2}{3}\begin{bmatrix} \cos(\sigma_s - \sigma) & \cos\left((\sigma_s - \sigma) - 2\pi/3\right) & \cos\left((\sigma_s - \sigma) - 4\pi/3\right) \\ -\sin(\sigma_s - \sigma) & -\sin\left((\sigma_s - \sigma) - 2\pi/3\right) & -\sin\left((\sigma_s - \sigma) - 4\pi/3\right) \\ 1/2 & 1/2 & 1/2 \end{bmatrix} \tag{2.29}$$

The voltage and flux linkage equations are given as follows (2.30)-(2.37). Here the subscript 's' denotes stator quantity and 'r' represents rotor quantity and all the rotor quantities are referred to the stator.

$$v_{ds} = r_s i_{ds} + \frac{d}{dt}\psi_{ds} - \omega_s\psi_{qs} \tag{2.30}$$

$$v_{qs} = r_s i_{qs} + \frac{d}{dt}\psi_{qs} + \omega_s\psi_{ds} \tag{2.31}$$

$$v_{dr} = r_r i_{dr} + \frac{d}{dt}\psi_{dr} - (\omega_s - \omega_r)\psi_{qr} \tag{2.32}$$

$$v_{qr} = r_r i_{qr} + \frac{d}{dt}\psi_{qr} + (\omega_s - \omega_r)\psi_{dr} \tag{2.33}$$

$$\psi_{ds} = L_s i_{ds} + L_m i_{dr} \tag{2.34}$$

$$\psi_{qs} = L_s i_{qs} + L_m i_{qr} \tag{2.35}$$

$$\psi_{dr} = L_r i_{dr} + L_m i_{ds} \tag{2.36}$$

$$\psi_{qr} = L_r i_{qr} + L_m i_{qs} \tag{2.37}$$

The equivalent circuit representation of dynamic model of induction machine in synchronous reference frame is shown in Fig. 2.5.
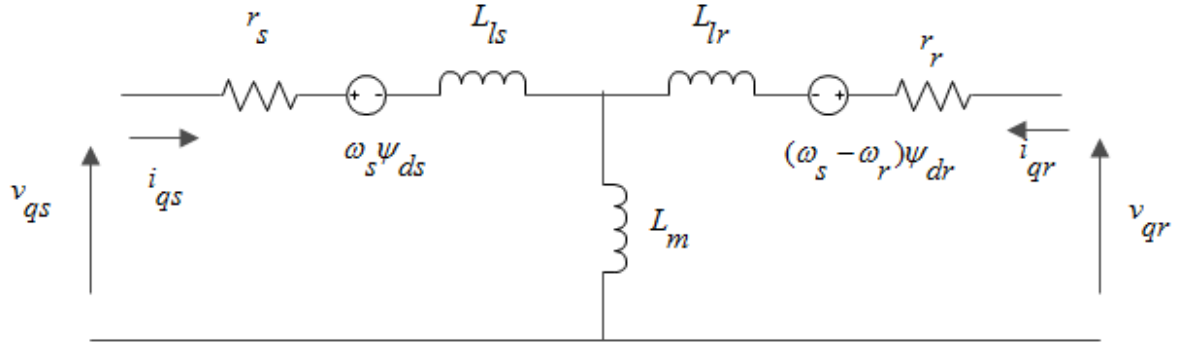

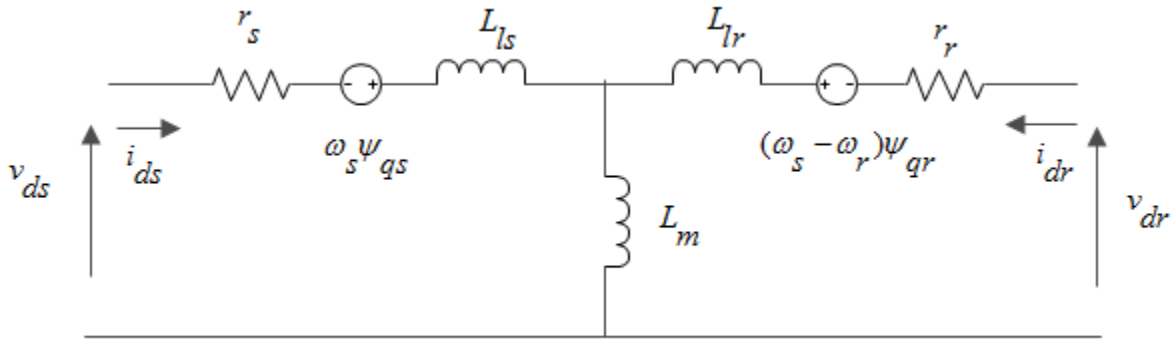Fig. 2.5(a) q-axis equivalent circuit of WRIM

Fig. 2.5(b) d-axis equivalent circuit of WRIM

In general the expressions for torque, active power and reactive power in dq synchronous reference frame are given in equations (2.38)-(2.40) as follows.

$$T_e = \psi_{dr}i_{qr} - \psi_{qr}i_{dr} \tag{2.38}$$

$$P_s = \frac{3}{2}(V_{qs}I_{qs} + V_{ds}I_{ds}) \tag{2.39}$$

$$Q_s = \frac{3}{2}(V_{qs}I_{ds} - V_{ds}I_{qs}) \tag{2.40}$$

18

OPEN LOOP CONTROL STRATEGY FOR DFIG BASED STAND-ALONE WECS

3.1 INTRODUCTION

The model of DFIG based stand-alone WECS with open loop control structure is shown in Fig. 3.1. There is a WRIM with two back to back VSC converters coupled with a common dc link capacitor. The two converters are named as stator side converter and rotor side converter. The stator converter terminals are connected to the stator terminals directly without any filter in between them. The rotor side converter is connected to the rotor terminals and the rotor shaft of the induction machine is driven by a prime mover as shown in Fig. 3.1. The load is connected at the capacitor filter junction which is in turn connected to the stator terminals via an inductive filter as shown in Fig. 3.1. Because of this inductive filter in between the load and stator terminals the model is expected to give poor load voltage regulation. Here the model works in two modes i.e. buildup of voltage at dc link capacitor and constant frequency generation mode.
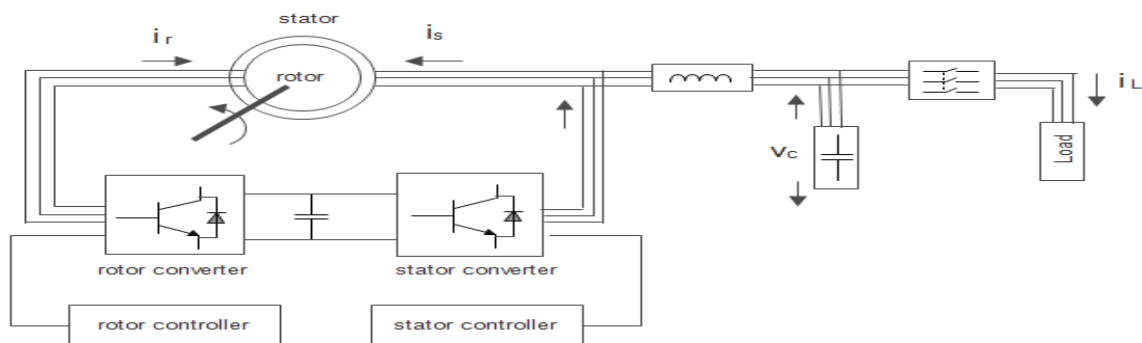

Fig. 3.1 Schematic of DFIG based WECS with open loop control strategy

Once as the voltage at the dc link capacitor terminals reaches up to the desired reference value thereafter the load should be connected for constant voltage and frequency maintenance. For achieving this, the load is connected at the filter capacitor junction via a three phase circuit breaker as shown in Fig. 3.1.

For this model the output voltage control is achieved in a direct voltage control manner which is implemented using the stator side converter where the reference voltage signals are generated in dq reference frame. The rotor converter is current controlled where the q-axis rotor current is used to control the power imbalance of the system and the direct axis component is left undisturbed after the dc link voltage reaches to its desired value. Both stator and rotor side converter controllers are modeled in dq reference frame which is forced to align with the stator flux linkage space vector.

Hence the dynamic model of the WRIM in stator flux oriented reference frame is considered for modelling the system. The equations that describe the dynamic model in stator flux reference frame are deduced as follows.

3.2 DYNAMIC MODEL OF INDUCTION MACHINE

The general voltage and flux linkage equations of slip ring induction machine in dq reference frame which rotates with a speed of ω_s rad/sec are given below.

$$v_{ds} = r_s i_{ds} + \frac{d}{dt}\psi_{ds} - \omega_s \psi_{qs} \tag{3.1}$$

$$v_{qs} = r_s i_{qs} + \frac{d}{dt}\psi_{qs} + \omega_s \psi_{ds} \tag{3.2}$$

$$v_{dr} = r_r i_{dr} + \frac{d}{dt}\psi_{dr} - (\omega_s - \omega_{r)}\psi_{qr} \tag{3.3}$$

$$v_{qr} = r_r i_{qr} + \frac{d}{dt}\psi_{qr} + (\omega_s - \omega_{r)}\psi_{dr} \tag{3.4}$$

$$\psi_{ds} = L_s i_{ds} + L_m i_{dr} \tag{3.5}$$

$$\psi_{qs} = L_s i_{qs} + L_m i_{qr} \tag{3.6}$$

$$\psi_{dr} = L_r i_{dr} + L_m i_{ds} \tag{3.7}$$

$$\psi_{qr} = L_r i_{qr} + L_m i_{qs} \tag{3.8}$$

Here all the rotor quantities are referred to the stator. Now for stator flux oriented reference frame it is certain that the quadrature axis flux is zero and the total flux is taken along the direct axis. i.e.

$$\psi_{qs} = \frac{d}{dt}\psi_{qs} = 0 \quad ; \quad \psi_{ds} = \psi_s \tag{3.9}$$

i.e. $\quad i_{ds} = \frac{\psi_s}{l_s} - \frac{l_m}{l_s} i_{dr} \quad ; \quad i_{qs} = -\frac{l_m}{l_s} i_{qr}$ \hfill (3.10)

Substituting the above relations in voltage and flux linkage equations (3.1)-(3.8) the following expressions are resulted which denotes the machine model in stator flux oriented reference frame [18].

- $v_{ds} = \frac{\psi_s}{\tau_s} - \frac{l_m}{\tau_s} i_{dr} + \frac{d}{dt}\psi_s$ \hfill (3.11)

- $v_{qs} = \omega_s \psi_s - \frac{l_m}{\tau_s} i_{qr}$ \hfill (3.12)

- $v_{dr} = l\frac{d}{dt} i_{dr} - l(\omega_s - \omega_r)i_{qr} + r_r i_{dr}$ \hfill (3.13)

- $v_{qr} = l\frac{d}{dt} i_{qr} + l(\omega_s - \omega_r)i_{dr} + (r_r i_{qr} + (\omega_s - \omega_r)\frac{l_m}{l_s}\psi_s)$ \hfill (3.14)

Where $\quad l = \frac{l_s l_r - l_m^2}{l_s} \quad$ and $\quad \tau_s = \frac{l_s}{r_s}$

From the above equations one can see that when the magnitude of stator flux and rotational frequency of the reference frame are maintained constant, the magnitude of stator voltage depends

only on the resistive drops which are negligible. Hence for maintaining constant voltage profile at stator terminals there is a necessity to control the magnitude of stator flux vector along with its rotational speed.

3.3 STATOR SIDE CONVERTER CONTROL

The block diagram of entire stator side converter control scheme is shown in Fig. 3.2.
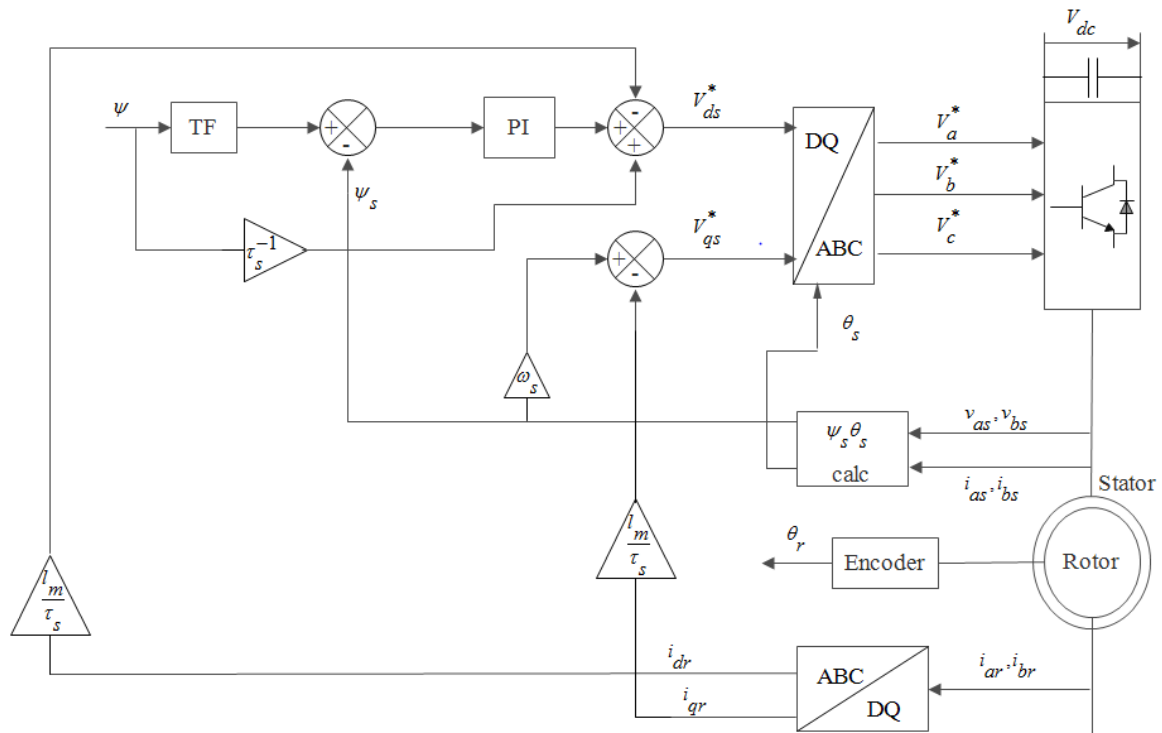

Fig. 3.2 Schematic of stator side converter control scheme

As mentioned in the introduction, stator side converter is voltage controlled where the quadrature axis and direct axis voltage components are generated as shown in the Fig. 3.2. The initial conditions and final conditions of dc link voltage build up process are mentioned as follows:

$$\omega_r = \omega_{rs} > 0, \qquad \omega_s = 0, \ \psi_s = 0, \qquad v_{dc} = Vdo > 0$$

$$\omega_r = \omega_{rs}, \qquad \omega_s = \omega_s^*, \quad \psi_s = \psi, \qquad v_{dc} = V_{dc}$$

The stator reference flux and actual flux are related by the following equation

$$\psi_s = \psi(1 - e^{-\frac{t}{t_s}}) \tag{3.15}$$

From the stator voltage equations (3.9), (3.10) and the above target conditions we get the stator voltage control variables as shown below [18].

$$v_{ds}^* = \frac{\psi}{t_s} - \frac{l_m}{t_s} i_{dr}^{\prime e} \quad and \quad v_{qs}^* = \omega_s^* \psi_s - \frac{l_m}{t_s} i_{qr}^{\prime e} \tag{3.16}$$

Two stator phase voltages and two stator phase currents are sensed which are converted in to stationary α-β components which are in turn used for the stator flux calculation and the unit vector generation as shown below.

$$v_{\alpha s} = r_s i_{\alpha s} + \frac{d}{dt} \psi_{\alpha s} \; ; \; v_{qs} = r_s i_{qs} + \frac{d}{dt} \psi_{qs} \tag{3.17}$$

$$\psi_s = \sqrt{(\psi_{\alpha s})^2 + (\psi_{\beta s})^2} \tag{3.18}$$

$$\cos \theta_s = \frac{\psi_{\alpha s}}{\psi_s} \quad ; \quad \sin \theta_s = \frac{\psi_{\beta s}}{\psi_s} \tag{3.19}$$

The rotor three phase currents are sensed and they are converted in to d-q component currents in reference frame which is oriented along the stator flux linkage vector, that are used for adding compensating currents as shown in Fig. 3.2. Finally the reference voltages generated in d-q reference frame are converted in to ABC reference frame using the unit vectors generated shown in equation (3.19) and from these voltages the modulating signals are deduced for sine PWM converter following the relation between the dc link voltage, fundamental component of output voltage, and the modulation index as explained in the following section.

3.4 SPWM TECHNIQUE

Sine PWM technique is employed here because of its simplicity and also it is easy to implement a sine triangular PWM technique compared to the Space Vector Pulse Width Modulation (SVPWM) technique. Also in terms of performance sine PWM technique is almost similar to that of a space vector PWM technique.
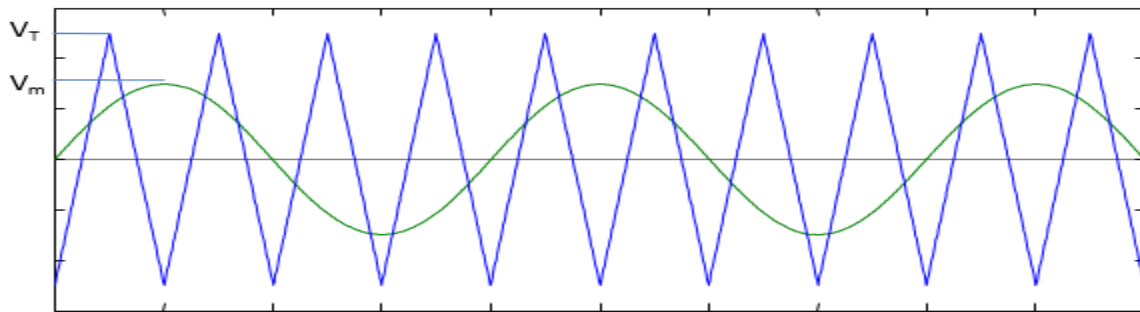

Fig. 3.3 Modulation signal of SPWM technique

For sine PWM inverter with V_d as dc input voltage and V_{ao} as the fundamental component of ac output voltage and m_i as modulating index that is defined as ratio of the magnitude of modulating signal to that of triangular carrier signal, the Fourier analysis of the output voltage gives the following relation.

$$V_{ao}=0.5m_iV_d \tag{3.20}$$

Where
$$m_i = \frac{v_{ma}}{v_T} \tag{3.21}$$

Therefore expression for modulating signal can be deduced as follows

$$v_{ma} = \frac{2v_T}{v_d} \tag{3.22}$$

24

This modulating signal is compared with triangular carrier wave of magnitude v_T as shown in Fig. 3.3 for generation of pulses which are fed to the switches of the stator side converter.

3.5 ROTOR SIDE CONVERTER CONTROL

As it is already mentioned the rotor side converter is current controlled where the q-axis component is used to nullify the power imbalance of the system through the dc link voltage controller which modifies the quadrature current component according to the changes in the dc link voltage. The schematic of the entire rotor converter control algorithm is shown in Fig. 3.4. Using the unit vectors generated as shown in equation (3.19) for reference frame transformation the rotor currents and stator currents are transformed in to their corresponding d-q axes components. The rotor flux calculation is done using the rotor flux linkage equations (3.7) and (3.8) as mentioned in the dynamic machine model. During the rise of dc link voltage at the capacitor terminals from a low initial value to the desired level, the rotor currents are generated following the relations shown in equation (3.23). During VSCF generation a dc link voltage controller comes in to picture which is used to generate the q-axis rotor current and the d-axis rotor current is left undisturbed during variable speed constant frequency generation. The difference between the actual dc link capacitor voltage sensed and the reference voltage is fed to the PI controller as shown in Fig. 3.4. Initially during the establishment of dc link voltage the rotor d-q current components are chosen as follows [18].

$$i_{dr}^* = I_{dr}^* \left(1 - e^{-\frac{t}{T_d}}\right) \; ; \; i_{qr}^* = I_{qr}^* \left(1 - e^{-\frac{t}{T_q}}\right) \qquad (3.23)$$

With the choice of these currents the dc link voltage gradually starts rising to its final reference value which is governed by equation (3.24).

$$\frac{C}{3}\frac{dv_d^2}{dt} = -(v_{qs}^{e*}i_{qi}^e + v_{ds}^{e*}i_{di}^e + v_{qr}'^e i_{qr}'^{e*} + v_{dr}'^e i_{qr}'^{e*}) \qquad (3.24)$$

Once the dc link voltage reaches its desired reference value the switch shown in Fig. 3.4 is used to connect the dc link voltage controller for generation of quadrature axis rotor current reference component. The rotor flux d-q components are calculated using the relations shown in equations (3.7) and (3.8) in section 3.2. These rotor flux components are used for calculating the compensating terms that are to be added for reference voltage generation as shown in the schematic diagram in Fig. 3.4.
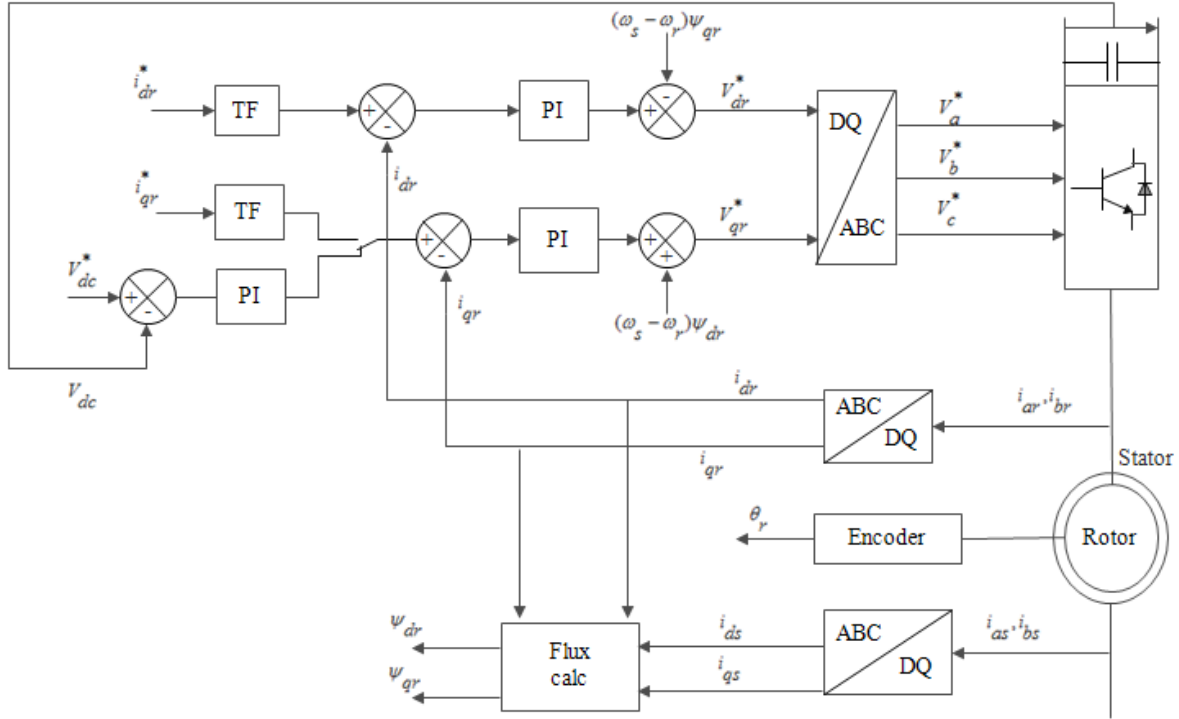
Fig. 3.4 Schematic of rotor side converter control scheme

The direct axis rotor reference current is left undisturbed in the VSCF generation mode. The difference between the reference values and actual values of the rotor currents is fed to the PI controllers for generation of the corresponding reference voltage components in d-q reference

frame. These voltages are converted in to ABC reference frame using the reference angle for transformation as shown in Fig. 3.5. From these reference voltages in ABC reference frame the modulating signals are deduced in similar manner as explained for stator side converter control. Finally the modulating signals are compared with triangular carrier waves for generation of pulses which are fed to the rotor converter switches. Once the system enters in to VSCF generation mode then only the load at the output terminals should be connected so that the system works satisfactorily.

The unit vectors generated for stator flux orientation which are governed by the equation (3.19) are shown below in Fig. 3.5(a) and Fig. 3.5(b).

Fig. 3.5(a) Unit vector sin (θ_s)

Fig. 3.5(b) Unit vector cos (θ_s)

3.6   SIMULATION RESUTLS AND DISCUSSION

In the simulated model the machine is rated at 5.6 kW and a load of 2.5 kW is considered. The simulated model is tested for load transients and speed changes and its transient performance is analyzed. First balanced linear load is considered and then nonlinear loads are concerned in the next step. An initial dc link capacitor voltage of 30 volts is applied. The load is applied at 0.5

seconds and the rotor speed is maintained constant at 110 rad/sec up to 0.7 seconds and from 0.7

to 0.9 seconds the rotor speed is dropped from 110 to 70 rad/sec and from 0.9 seconds it is again

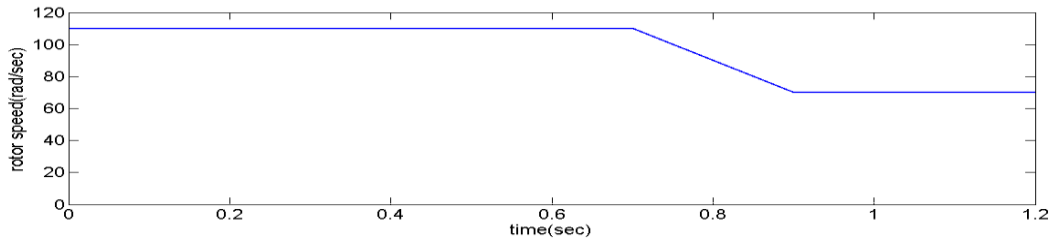maintained constant which is shown in Fig. 3.6.

Fig. 3.6 Rotor speed

The direct axis and quadrature axis rotor current components are shown in Fig. 3.7 from which it

is clear that the q-axis current is changed from nearly zero to 10 amp at 0.5 seconds due to load

transient and again changes from 10 to 15 amperes during speed change which clearly shows that

dc link voltage controller commands the q-axis reference current.
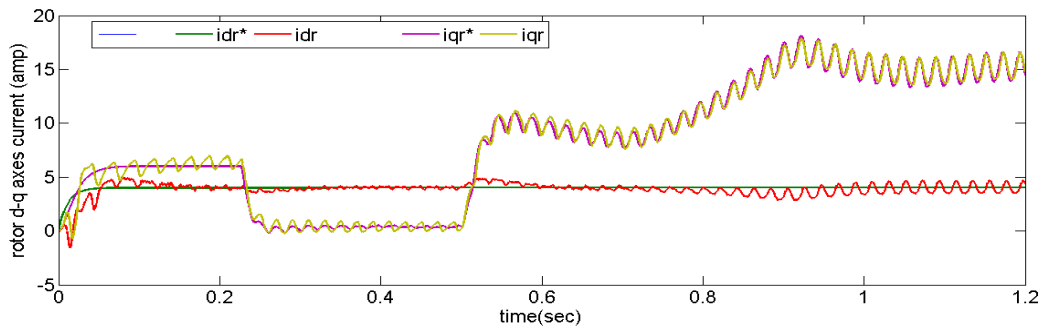
Fig. 3.7 Rotor current in synchronous frame.

The dc link voltage profile is shown below in Fig. 3.8 from which it is clear that at 0.5 seconds as

the load is suddenly applied there is power imbalance due to which there is a slight dip in dc link

voltage and then it regains to its reference value as q-axis rotor current is increased accordingly.

Also from 0.7 to 0.9 seconds as the rotor speed is reduced there is again a slight dip in dc link voltage profile which again regains its reference value due to increase in q-axis rotor current.
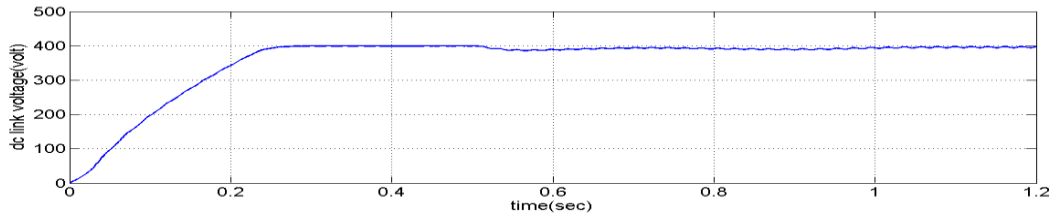
Fig. 3.8 dc link voltage profile

The load current waveform and load voltage waveform during load transients are shown in Fig. 3.9 and Fig. 3.10 respectively along with the FFT analysis of the load voltage which is shown in Fig. 3.11. It is clear from Fig. 3.10 that there is a slight reduction in magnitude of load voltage after the application of load at 0.5 seconds.
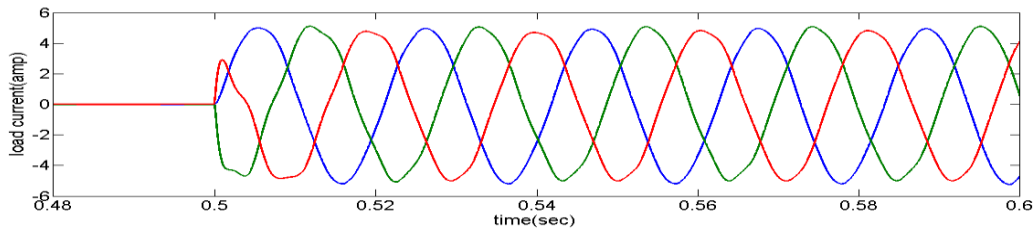
Fig. 3.9 Load current
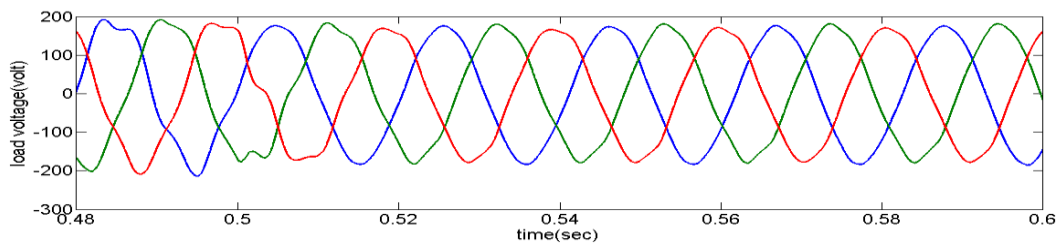
Fig. 3.10 Load voltage profile
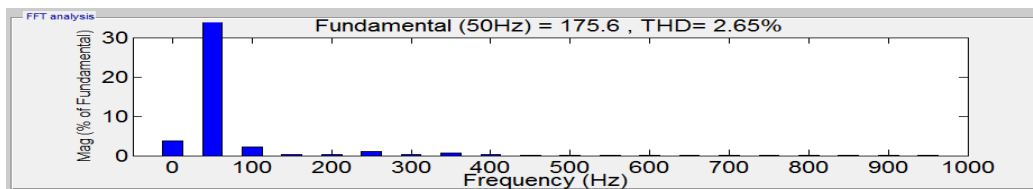
Fig. 3.11 FFT analysis of load voltage

29

The stator flux wave form along with d-q axes reference voltages generated from the stator side converter control scheme are show in Fig. 3.12 and Fig. 3.13. From the graph in Fig. 3.12 it is clear that the actual flux is aligned whit the reference stator flux which is 0.574 Weber's.
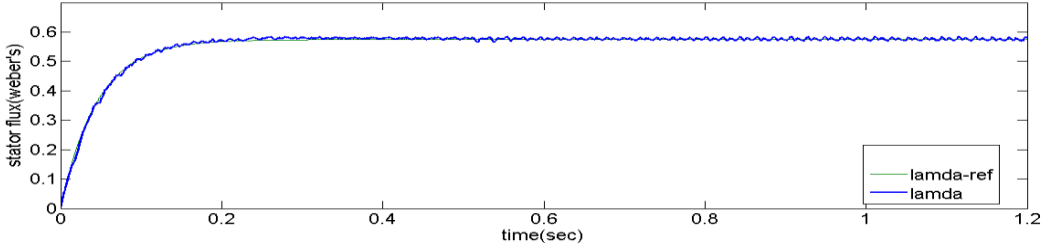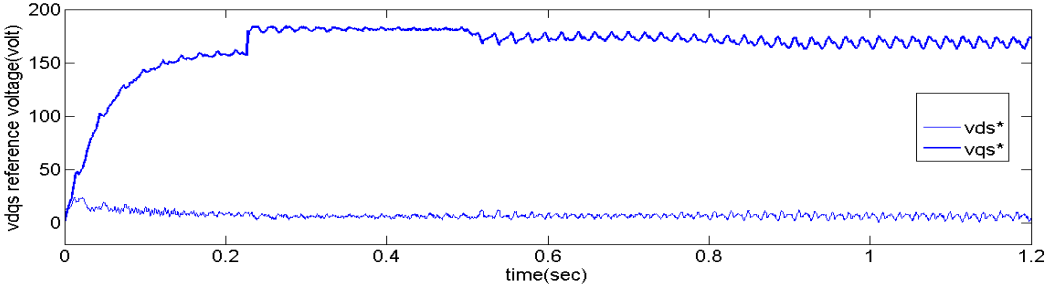

Fig. 3.12 Stator flux

Fig. 3.13 Stator voltage in synchronous frame

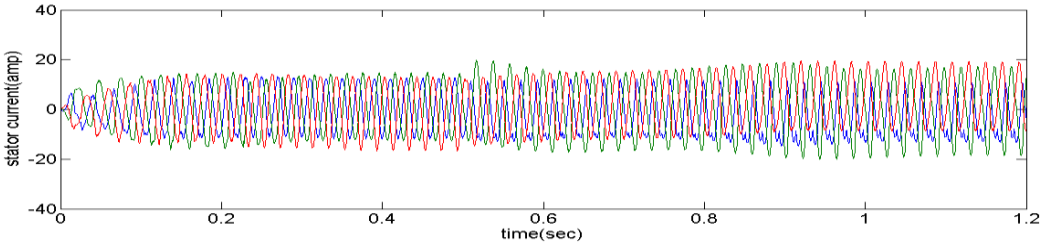The stator current profile is shown in Fig. 3.14 and its FFT analysis is shown in Fig. 3.15.
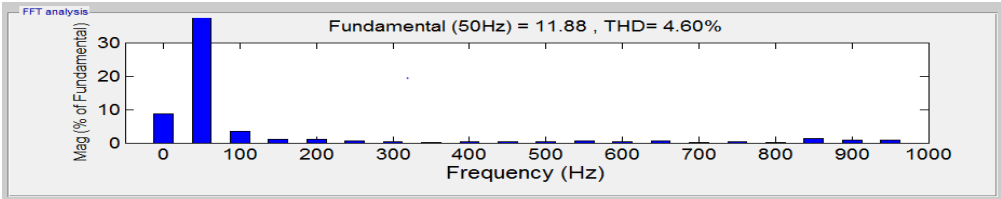

Fig. 3.14 Stator current

Fig. 3.15 FFT analysis of stator current

The load voltage profile for application of nonlinear load is shown in Fig. 3.16. The load current profile and FFT analysis of load voltage are shown in Fig. 3.17 and Fig. 3.18 respectively for the application of three phase nonlinear load which is a three phase diode rectifier circuit feeding an R-L load.
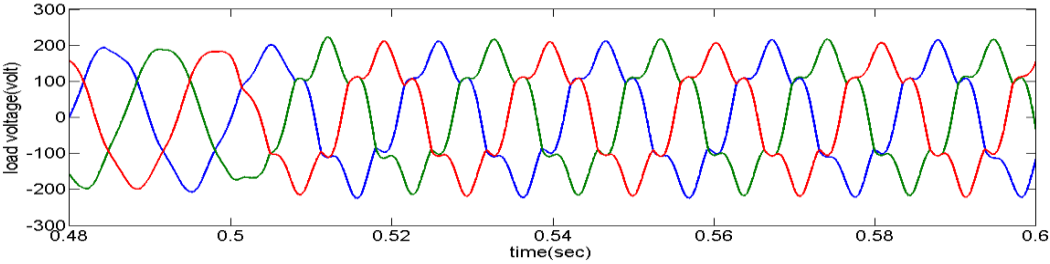

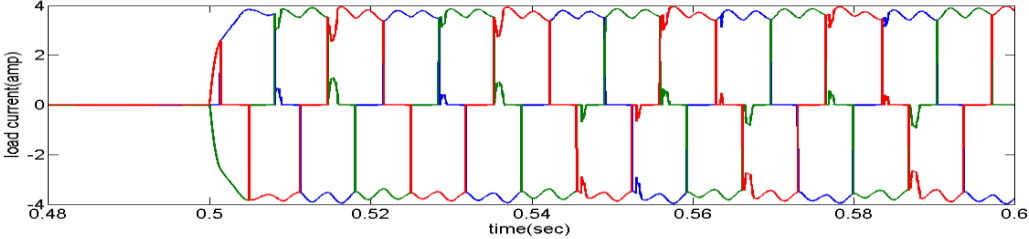Fig. 3.16 Load voltage for nonlinear load (open loop control)

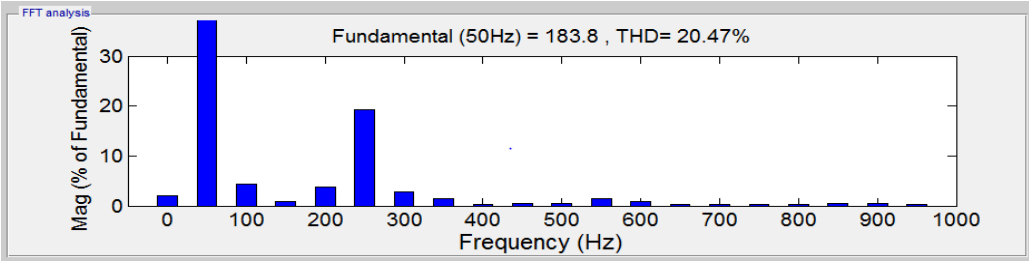Fig. 3.17 Load current for nonlinear load

Fig. 3.18 FFT analysis of load voltage for nonlinear load (open loop control)

From the load voltage waveform shown in Fig. 3.16 it is clear that there are unwanted distortions in the load voltage with the application of nonlinear load.

Thus the open loop control strategy implemented in this model is not suitable for nonlinear loads and unbalanced nonlinear loads as well.

Hence a closed loop control structure is implemented in the following chapter which works satisfactorily for all loads (balanced, unbalanced, linear, nonlinear and unbalanced nonlinear).

CLOSED LOOP CONTROL STRATEGY FOR DFIG BASED STAND-ALONE WECS

4.1 INTRODUCTION

The schematic of the DFIG based stand-alone WECS with closed loop control strategy is shown in Fig. 4.1. It consists of a WRIM with two PWM converters connected in back to back configuration and are coupled with a common dc link capacitor. The rotor of the machine is connected to a prime mover. The two converters are named as stator converter and rotor converter respectively. Ac side of the stator converter is connected to the machine stator terminals via an inductive filter as show in Fig. 4.1. A capacitive filter is connected at the junction to which load terminals are connected through a switch. The only difference between the configurations adopted for open loop scheme and that of closed loop scheme is that of the placement of inductive filter. In the present configuration as the inductive filter is placed in between the machine stator terminals and stator converter terminals it is expected to give good voltage regulation at the output terminals as the load is connected to the stator terminals at the capacitor filter junction without any inductive filter between the load and stator terminals. The control algorithm used for this configuration is same as that of open loop control structure except an additional stator voltage control strategy is implemented in the stator side converter control. The stator converter is voltage controlled converter where the difference between the reference voltage and actual voltage is fed to stator voltage controller that accordingly modifies the reference inverter output voltages.
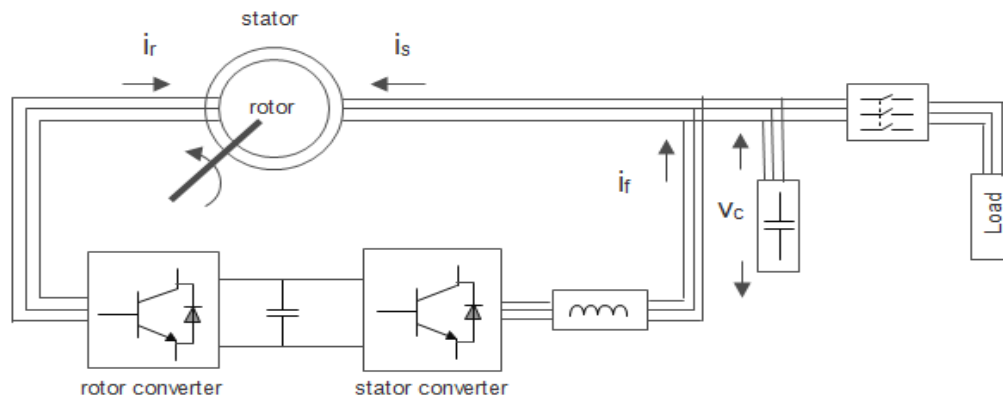
Fig. 4.1 Schematic of DFIG based stand-alone system with closed loop control scheme

The rotor converter is current controlled where the quadrature axis rotor reference current is generated using a dc link voltage controller so that it maintains the power balance of the system. Whenever there is any power imbalance in the system the corresponding change will be reflected in the dc link capacitor voltage. For example when there is sudden increase in the load there will be a fall in the dc link voltage and accordingly the quadrature axis rotor current is forced to increase so that torque will increase which increases the total output power and nullifies the power imbalance in the entire system. In this manner whenever there are load changes and speed changes, the q-axis rotor current will be adjusted accordingly so that power balance is maintained. The entire rotor side converter control is similar to that explained in third chapter for open loop control strategy and its block diagram is shown in Fig. 3.4. Hence in the current chapter a major focus will be given on stator voltage controller as follows.

4.2   STATOR SIDE CONVERTER CONTROL

The stator reference voltages are generated according to the equation (3.16) given in chapter 3 and the entire schematic of stator side converter is also shown in Fig. 3.2 in chapter 3. Now in this closed loop control scheme the capacitor filter is forced to maintain these reference voltages generated and this process is achieved by means of a stator voltage controller. Before having a deep insight in to this stator voltage controller there is a need to represent the stator side inverter along with inductive filter in dq synchronous reference frame and is shown below. The direct axis and quadrature axis equivalent circuits of stator side inverter along with filter are shown in Fig. 4.2 and Fig. 4.3 respectively.
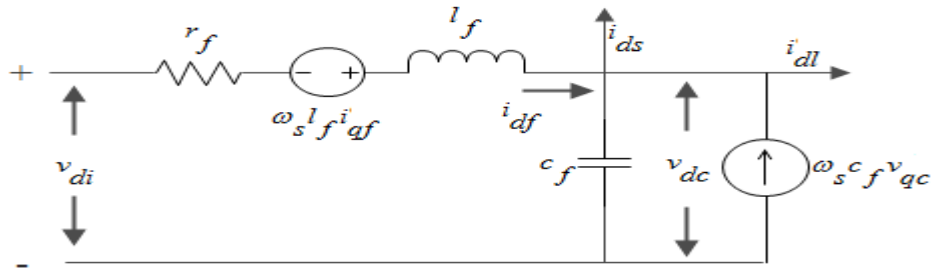

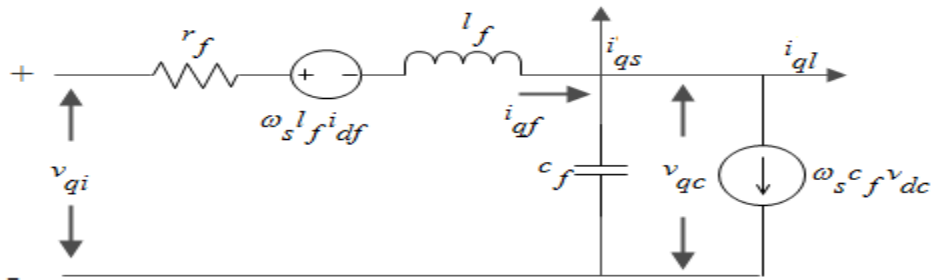Fig. 4.2 equivalent circuit in d-axis.

Fig. 4.3 equivalent circuit in q-axis

35

The voltage and current equations governing the d-q axes equivalent circuits expressed in synchronous reference frame are as follows [18]:

$$c_f \frac{d}{dt} v_{dc} = i_{df} - i_{dl} - i_{ds} + \omega_s c_f v_{qc} \tag{4.1}$$

$$c_f \frac{d}{dt} v_{qc} = i_{qf} - i_{ql} - i_{qs} - \omega_s c_f v_{dc} \tag{4.2}$$

$$v_{di} = r_f i_{df} + l_f \frac{d}{dt} i_{df} - \omega_s l_f i_{qf} + v_{dc} \tag{4.3}$$

$$v_{qi} = r_f i_{qf} + l_f \frac{d}{dt} i_{qf} + \omega_s l_f i_{df} + v_{qc} \tag{4.4}$$

As the capacitor terminals are directly connected to the machine stator terminals the voltage at the capacitor terminals is same as that of the stator voltage and hence it can be written as follows.

$$v_{dc} = v_{ds} \quad and \quad v_{qc} = v_{qs} \tag{4.5}$$

The schematic of stator voltage controller is shown in Fig. 4.4. The two phase quantities of stator voltage, stator current, filter current, and load current are sensed and are transformed in to their corresponding d-q quantities in synchronously rotating reference frame using the unit vector signals shown in equation (3.19) for transformation. All these quantities are fed to the stator voltage controller along with the stator d-q axes reference voltages whose generation is already explained in the previous chapter. The stator voltage controller generates the reference voltage signals for stator side inverter in synchronous reference frame after adding the compensating terms which are as shown in the schematic diagram of stator voltage controller in Fig. 4.4.
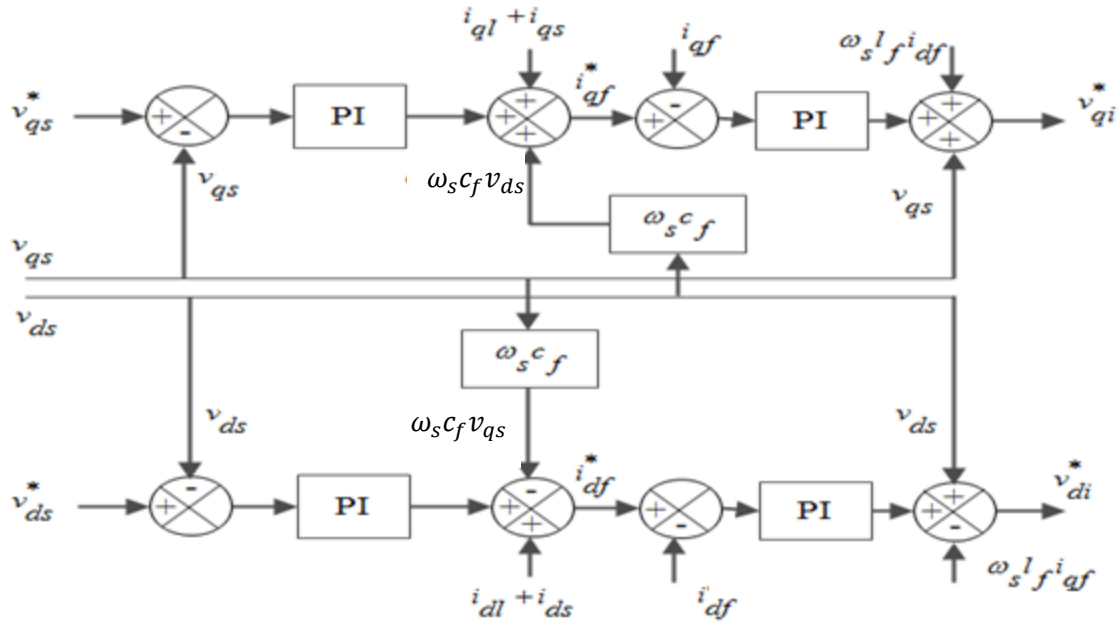
Fig. 4.4 Schematic of stator voltage controller [18].

The reference voltages for stator side inverter in synchronously rotating reference frame are then transformed in to three phase quantities expressed in ABC reference frame. These reference signals generated are processed to get the modulation signals for sine PWM technique which are compared with triangular carrier waves for generation of pulses. These pulses are then fed to the switches of the stator side converter.

4.3 SIMULATION RESULTS AND DISCUSSION

In the simulated model the machine is rated at 5.6 kW and a load of 2.5 kW is considered. The simulated model is tested for load transients and speed changes and its transient performance is analyzed. First balanced linear load is considered and then nonlinear loads are concerned in the next step. An initial dc link capacitor voltage of 30 volts is applied. The load is applied at 0.5 seconds and the rotor speed is maintained constant at 110 rad/sec up to 0.7 seconds and from 0.7

to 0.9 seconds the rotor speed is dropped from 110 to 70 rad/sec and from 0.9 seconds it is again maintained constant as already shown in Fig. 3.6.

The dc link voltage profile is shown in Fig. 4.5 having a transient at 0.5 sec due to sudden application of load and the rotor current in synchronous reference frame is shown in Fig. 4.6 where the q-axis rotor current rises at 0.5sec due to load change and also from 0.7 to 0.9 sec it increases linearly to compensate fall in speed accordingly.
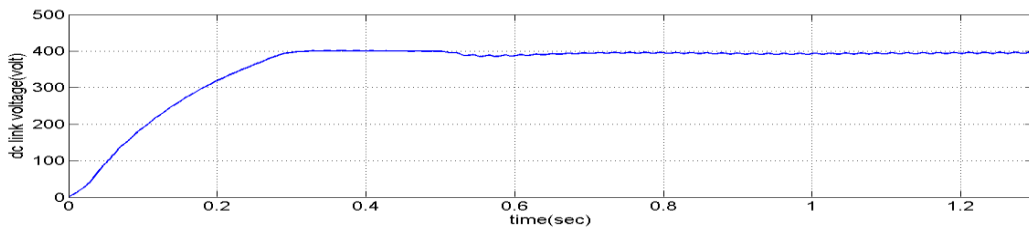

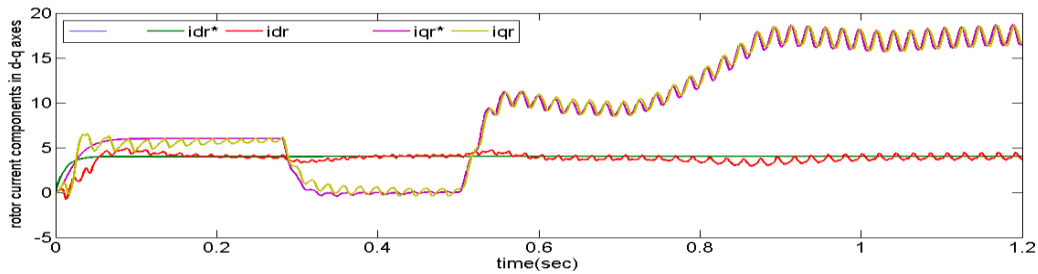Fig. 4.5 dc link voltage profile

Fig. 4.6 Rotor current in synchronous reference frame

The stator flux and stator voltage in synchronous reference frame are shown in Fig. 4.7 and Fig. 4.8 where the actual values are forced to align with the reference values by the controller action.
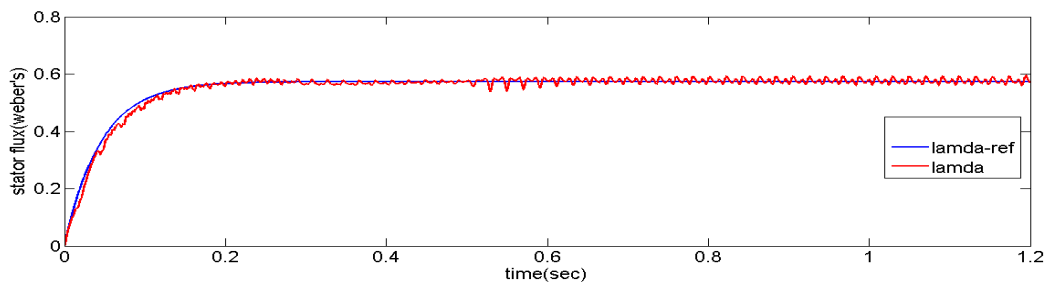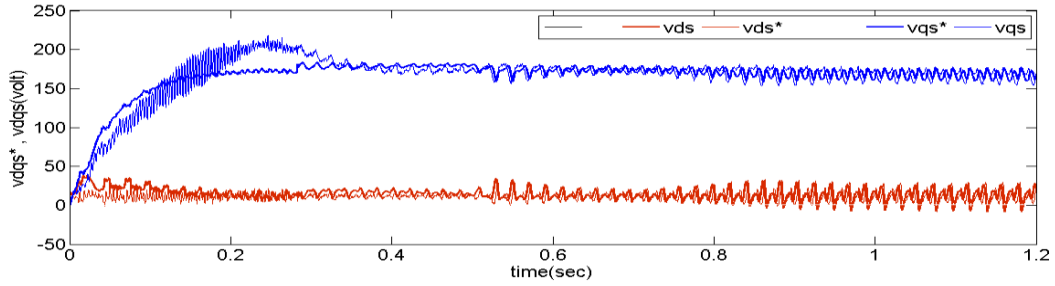

Fig. 4.7 Stator flux

38

Fig. 4.8 Stator voltage in synchronous reference frame

The stator current, load current and load voltage profiles are shown in Fig. 4.9, Fig. 4.10 and Fig. 4.11 respectively. From the load voltage profile it is clear that there is negligible voltage drop at the load terminals during sudden application of the load at 0.5 sec which shows that this model exhibits good load voltage regulation compared to the one with open loop control scheme.
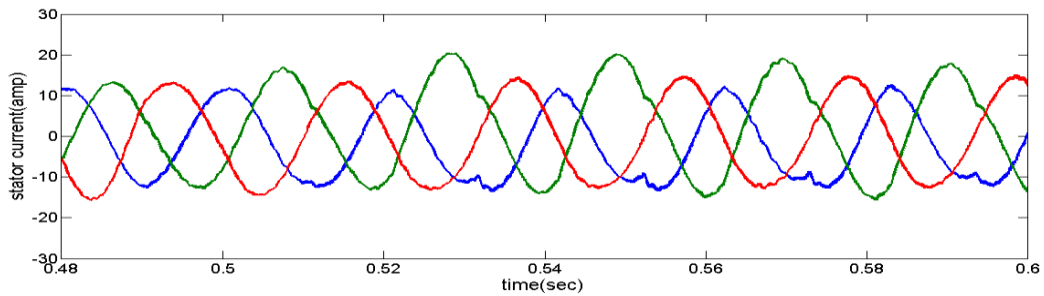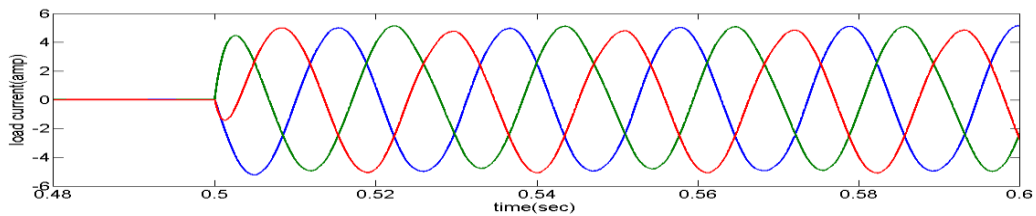

Fig. 4.9 Stator current
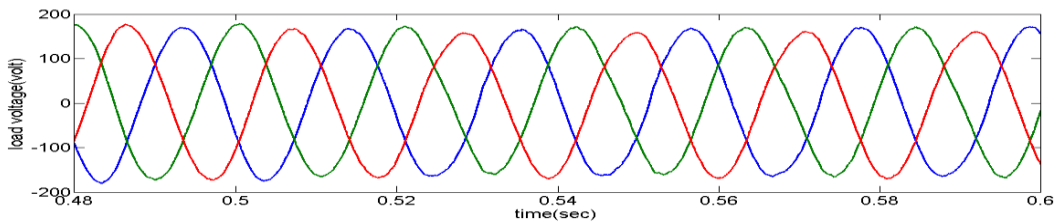

Fig. 4.10 Load current

Fig. 4.11 Load voltage

39

Now the model is tested for a balanced nonlinear load which is nothing but a three phase diode rectifier supplying an R-L load. The load current is shown in Fig. 4.13. The stator current along with its FFT analysis is shown in Fig. 4.14 and in Fig. 4.15 respectively.
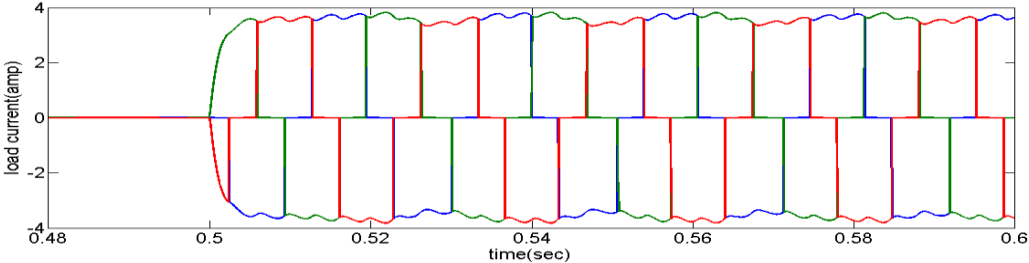

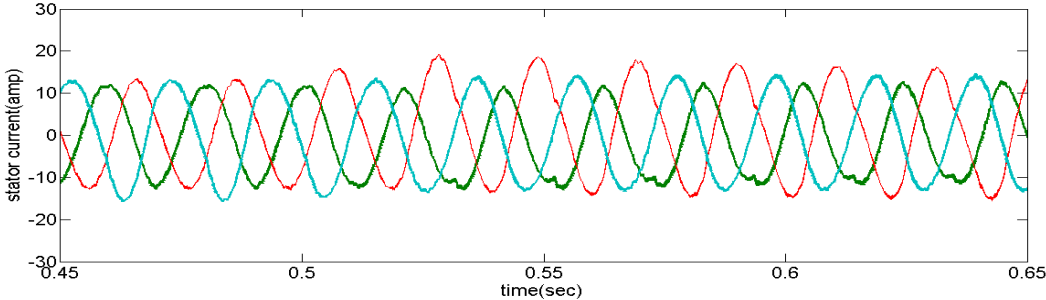Fig. 4.12 Load current for nonlinear load

Fig. 4.13 Stator current
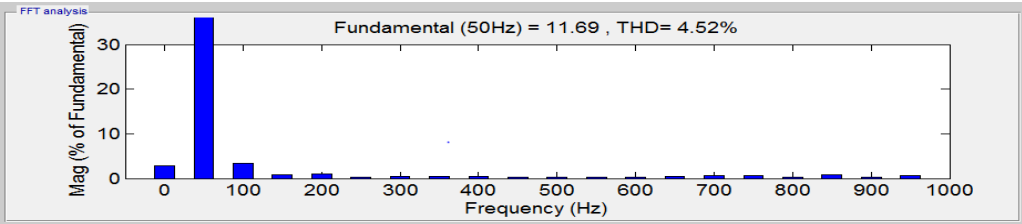
Fig.4.14 FFT analysis of stator current
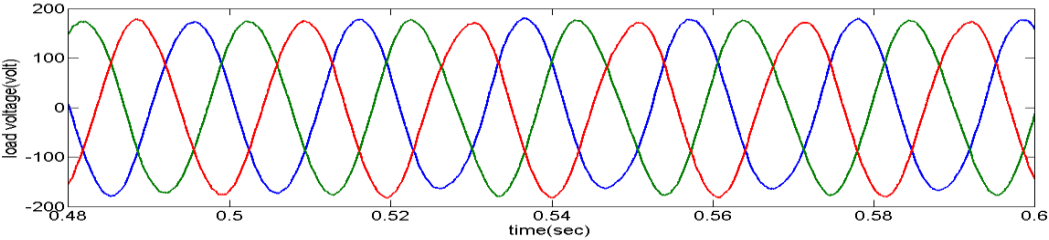
Fig. 4.15 Load voltage profile for nonlinear load (closed loop control)

40
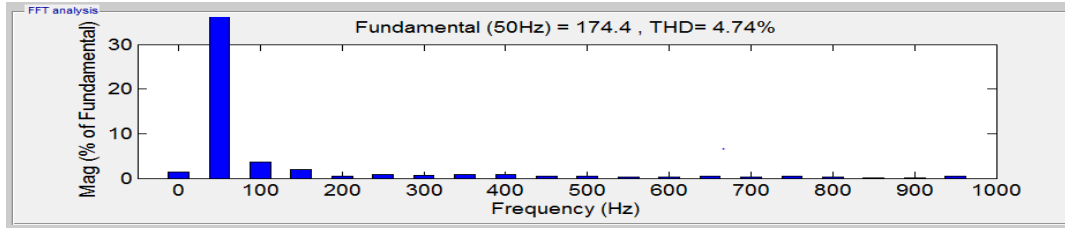
Fig. 4.16 FFT analysis of load voltage for nonlinear load (closed loop control)

The load voltage profile and its FFT analysis during load transient is shown in Fig. 4.16 and Fig. 4.17 respectively. From the load voltage profile shown in Fig. 4.16 it is clear that this model works satisfactorily for nonlinear loads and also there are no unwanted distortions in the load voltage unlike that of the model with open loop control scheme as explained in the previous chapter.

CHAPTER 5

CONCLUSIONS AND FUTURE SCOPE

The wound rotor induction machine dynamic models in different reference frames are studied and analyzed as a clear understanding is required for developing control algorithms for DFIG based stand-alone WECS. Two control algorithms are developed for two different configurations for achieving the desired objectives. One is open loop control scheme and the other is closed loop control structure. In the open loop control scheme a constant voltage magnitude and constant frequency is maintained at the output terminals and its transient performance is analyzed during sudden load transients and prime mover speed changes. But with this open loop scheme the following problems are encountered which enhances the need for closed loop control strategy.

- Poor load voltage regulation at the output terminals.

- Unwanted distortions are coming in to picture in load voltage profile for the application of nonlinear loads. Therefor this scheme is suitable only for balanced linear loads and it cannot be used for other categories of load.

In the closed loop control scheme a slight modification is done in the configuration and a direct stator voltage controller is added in the stator side converter control and this scheme is able to maintain all the desired qualities which are mentioned below.

- Maintaining constant magnitude and constant frequency voltage profile at the output terminals against the load transients and prime mover speed changes.

- Good load voltage regulation at the output terminals.

- Satisfactory operation for all types of loads which may be linear, nonlinear and unbalanced nonlinear loads as well.

FUTURE SCOPE

Some interesting areas for further studies are as follows.

- Hardware implementation of the model with closed loop control strategy using Field-Programmable Gate Array (FPGA).
- Modelling of DFIG based stand-alone WECS along with battery storage.
- Application of matrix converters in DFIG based wind energy conversion system as they are capable of ac to ac conversion.
- Study of grid connected operation of DFIG based WECS.

REFERENCES

[1]   Protsenko, Kostyantyn, and Dewei Xu, "Modeling and Control of Brushless Doubly-Fed Induction Generators in Wind Energy Applications'', *IEEE Transactions on Power Electronics,* Vol. 23, No. 3, pp. 1191-1197, May 2008.

[2]   Ekanayake, Janaka B., Lee Holdsworth, XueGuang Wu, and Nicholas Jenkins, "Dynamic Modeling of Doubly Fed Induction Generator Wind Turbines'', *IEEE Transactions on Power Systems,* Vol. 18, No. 2, pp. 803-809, May 2003.

[3]   Erlich, Istvan, Jorg Kretschmann, Jens Fortmann, Stephan Mueller-Engelhardt, and Holger Wrede, "Modeling of Wind Turbines Based on Doubly-Fed Induction Generators for Power System Stability Studies", *IEEE Transactions on Power Systems,* Vol. 22, No. 3, pp. 909-919, August 2007.

[4]   Luna, Alvaro, FK de A. Lima, David Santos, Pedro Rodríguez, Edson H. Watanabe, and Santiago Arnaltes, "Simplified Modeling of a DFIG for Transient Studies in Wind Power Applications", *IEEE Transactions on Industrial Electronics,* Vol. 58, No. 1, pp. 9-20, January 2011.

[5]   Torbjörn Thiringer and Jorma Luomi, "Comparison of Reduced-Order Dynamic Models of Induction Machines", *IEEE Transactions on Power Systems*, Vol.16, No. 1, pp. 119-126, February 2001.

[6]   Gill G. Richards and Owen T. Tan, "Simplified Models for Induction Machine Transients under Balanced and Unbalanced Conditions*", IEEE Transactions on Industry Applications*, Vol. IA-17, No. 1, pp. 15-21, January 1981.

[7]   Rodríguez, José R., Juan W. Dixon, José R. Espinoza, Jorge Pontt, and Pablo Lezana, "PWM Regenerative Rectifiers: State of the Art", *, IEEE Transactions on Industrial Electronics,* Vol. 52, No. 1, pp. 5-22, February 2005.

[8]   Guo, Yan, Xiao Wang, Howard C. Lee, and Boon-Teck Ooi, "Pole-placement Control of Voltage-regulated PWM Rectifiers through Real-time Multiprocessing", *IEEE Transactions on Industrial Electronics,* Vol. 41, No. 2, pp. 224-230, April 1994.

[9]   Blasko, Vladimir, and Vikram Kaura, "A New Mathematical Model and Control of a Three-phase AC-DC Voltage Source Converter", *IEEE Transactions on Power Electronics,* Vol. 12, No. 1, pp. 116-123, January 1997.

[10]   Kwon, Bong-Hwan, Jang-Hyoun Youm, and Jee-Woo Lim, "A Line-Voltage-Sensorless Synchronous Rectifier", *IEEE Transactions on Power Electronics,* Vol.14, No. 5, pp. 966-972, September 1999.

[11]   Pena, R., J. C. Clare, and G. M. Asher, "Doubly Fed Induction Generator using back-to-back PWM Converters and its Application to Variable-Speed Wind-Energy Generation." *IEE Proceedings-Electric Power Applications,* Vol. 143, No. 3, pp. 231-241, May 1996.

[12]   Xu, Longya, and Wei Cheng, "Torque and Reactive Power Control of a Doubly Fed Induction Machine by Position Sensorless Scheme", *IEEE Transactions on Industry Applications,* Vol. 31, No. 3, pp. 636-642, 1995.

[13] Datta, Rajib, and V. T. Ranganathan, "A Simple Position-Sensorless Algorithm for Rotor-side Field-oriented Control of Wound-rotor Induction Machine", *IEEE Transactions on Industrial Electronics,* Vol. 48, No. 4, pp. 786-793, 2001.

[14] Pena, R., J. C. Clare, and G. M. Asher, "A Doubly Fed Induction Generator using back-to-back PWM Converters Supplying an Isolated Load from a Variable Speed Wind Turbine", *IEE Proceedings- Electric Power Applications,* Vol. 143, No. 5, pp. 380-387, September 1996.

[15] Iwanski, Grzegorz, and Wlodzimierz Koczara, "Sensorless direct Voltage Control of the Stand-alone Slip-ring Induction Generator", *IEEE Transactions on Industrial Electronics,* Vol. 54, No. 2, pp. 1237-1239, 2007.

[16] Iwanski, Grzegorz, and Wlodzimierz Koczara, "DFIG-based Power Generation System with UPS function for Variable-Speed applications", *IEEE Transactions on Industrial Electronics,* Vol. 55, No. 8, pp. 3047-3054, August 2008.

[17] Isha, T. B., and D. Kastha, "Transient Performance of a Stand-alone Variable Speed Constant Frequency Generation System", *Power Conversion Conference-Nagoya*, pp. 622-628, April 2007.

[18] Pattnaik, M., and D. Kastha, "Control of Double Output Induction Machine Based Stand-alone Variable Speed Constant Frequency Generator with Nonlinear and Unbalanced Loads", *Power and Energy Society General Meeting,* pp. 1-8, 2010.

[19] Abram Perdana, "Dynamic Models of Wind Turbines", Ph.D. dissertation, Chalmers University of Technology, Sweden, 2008.

[20] Bimal K Bose, "Power electronics and motor drives", Academic press, 2010.

[21] Peter vas, "Vector control of AC machines", Oxford University Press, 1990.